# Analysis and suppression of nonlinear frequency modulation in an optical frequency-domain reflectometer

**Kivilcim Yüksel, Marc Wuilpart, and Patrice Mégret**

*Faculty of Engineering, Mons, Electromagnetism and Telecommunication Department, Boulevard Dolez 31, 7000-BE Mons, Belgium*

*kivilcim.yuksel@fpms.ac.be*

**Abstract:** A new method for monitoring the nonlinearities perturbing the optical frequency sweep in high speed tunable laser sources is presented. The swept-frequency monitoring system comprises a Mach-Zehnder interferometer and simple signal processing steps. It has been implemented in a coherent optical frequency domain reflectometer which allowed to drastically reduce the effects of nonlinear sweep, resulting to a spatial resolution enhancement of 30 times.



**OCIS codes:** (060.2300) Fiber measurements; (120.2920) Homodyning; (120.3180) Interferometry; (120.3940) Metrology

## References and links

1. J. Martins-Filho, C. Bastos-Filho, M. Carvalho, M. Sundheimer, and A. Gomes, "Dual-Wavelength (1050nm + 1550 nm) Pumped Thulium-Doped Fiber Amplifier Characterization by Optical Frequency-Domain Reflectometer," IEEE Photon. Technol. Lett. **15**, 24–26 (2003).
2. B. Soller, S. Kreger, D. Gifford, M. Wolfe, and M. Froggatt, "Optical Frequency Domain Reflectometry for Single- and Multi-Mode Avionics Fiber-Optics Applications," in *Avionics Fiber-Optics and Photonics, 2006*, pp. 38–39 (2006).
3. C. Ndiaye, T. Hara, and H. Ito, "Profilometry using a frequency-shifted feedback laser," in *Proceedings Conference on Lasers and Electro-Optics (CLEO)*, pp. 1757–1759 (CThM2) (Baltimore, Maryland, 2005).
4. H. Lim, J. de Boer, B. Park, E. Lee, R. Yelin, and S. Yun, "Optical frequency domain imaging with a rapidly swept laser in the 815-870 nm range," Opt. Express **14**, 5937–5944 (2006).
5. J. Zheng, "Analysis of optical frequency-modulated continuous-wave interference," Appl. Opt. **43**, 4189–4197 (2004).
6. U. Glombitza and E. Brinkmeyer, "Coherent Frequency-Domain Reflectometry for Characterization of Single-Mode Integrated-Optical Waveguides," J. Lightwave Technol. **11**, 1377–1384 (1993).
7. J. B. Soller, D. Gifford, M. Wolfe, and M. Froggatt, "High resolution optical frequency domain reflectometry for characterization of components and assemblies," Opt. Express **13**, 666–674 (2005).
8. T.-J. Ahn, J. Lee, and D. Kim, "Suppression of nonlinear frequency sweep in an optical frequency-domain reflectometer by use of Hilbert transformation," Appl. Opt. **44**, 7630–7634 (2005).
9. K. Tsuji, K. Shimizu, T. Horiguchi, and Y. Koyamada, "Spatial-resolution improvement in long-range coherent optical frequency domain reflectometry by frequency-sweep linearisation," Electron. Lett. **33**, 408–410 (1997).
10. T.-J. Ahn and D. Kim, "Analysis of nonlinear frequency sweep in high-speed tunable laser sources using self-homodyne measurement and Hilbert transformation," Appl. Opt. **46**, 2394–2400 (2007).
11. E. Moore and R. McLeod, "Correction of sampling errors due to laser tuning rate fluctuations in swept-wavelength interferometry," Opt. Express **16**, 13,139–13,149 (2008).
12. K. Tsuji, K. Shimizu, T. Horiguchi, and Y. Koyamada, "Coherent Optical Frequency Domain Reflectometry Using Phase-Decorrelated Reflected and Reference Lightwaves," J. Lightwave Technol. **15**, 1102–1109 (1997).

#107227 - $15.00 USD Received 5 Feb 2009; revised 24 Mar 2009; accepted 25 Mar 2009; published 26 Mar 2009

## 1. Introduction

Optical frequency-domain reflectometry (OFDR) has found a great number of applications, typically as a diagnostic and characterization tool for optical fibers, components and systems. It was then implemented for the measurement of distributed gain in optical amplifiers [1] and for the realization of distributed fiber optic temperature and strain sensors [2]. The OFDR was also adapted for the imaging of manufactured products [3] and biological tissues [4].

The basic phenomenon behind the coherent OFDR is the frequency-modulated continuous-wave (FMCW) interference (beating) which was originally investigated in electric radar systems [5]. In the basic configuration, the coherent OFDR consists of a tunable laser source (TLS) whose frequency can be swept continuously in time without mode hops and an optical interferometer comprising a reference path and a measurement path. The device under test (DUT) is connected to the measurement path whereas the reference path is used as local oscillator. The interferences between the reference signal from reference path and different reflections coming from the DUT is electrically detected and a Fourier transform allows the visualization of beat frequencies. If the optical frequency of the TLS is modulated at a constant rate, beat frequencies are proportional to the optical path differences between the reflections in the DUT and the reference path.

The key point of OFDR implementations is the requirement for high performance optical sources providing a fast and linear frequency tuning over a broad frequency range. However, the available lasers exhibit in practice fluctuations in their optical frequency tuning rate. Due to these nonlinear tuning characteristics, sampling of the interference signal with a constant spacing in time gives rise to a non-uniform sampling in optical frequency which, in turn, degrades the spatial resolution of the OFDR measurement. It is well known that this problem can be avoided by sampling the interference signal at equidistant instantaneous optical frequency points rather than equally spaced time intervals [6]. The commonly implemented approach is to monitor the time varying optical frequency simultaneously by means of an auxiliary interferometer. The zero crossing points of the signal at the detector output of the auxiliary interferometer are used to generate trigger pulses which are then used as an external sampling clock on the DUT interferometer. This method which is known as frequency sampling has however a major drawback: the maximum DUT length is limited by the path difference of the auxiliary interferometer in order to satisfy Nyquist theorem [6, 7].

Another approach uses an auxiliary interferometer as in the previous frequency sampling method but entails the suppression of nonlinear optical frequency sweep after data acquisition. In this approach the length limitation of the auxiliary interferometer is overcome [8]. The auxiliary interferometer is used to monitor the optical frequency of the TLS. Then, this information is used for re-sampling of the interference signal with an accurate equidistant optical frequency grid. The optical frequency versus time would be deduced from the interference fringes of the auxiliary interferometer output either by the way of electrical circuits (hardware) [9] or by using mathematical manipulations (software). Recently reported Hilbert transform compensation method is a good example for the latter option [8, 10]. In this method however, the need of phase-unwrapping used to obtain the phase of the detected light requires complex numerical algorithms.

In this paper we describe a new method to measure the optical frequency of a commercial tunable laser source by using an auxiliary interferometer and some simple signal processing steps. The time varying phase of the beat signal from a self-homodyne interferometer is first converted to an amplitude change. The envelope detection of this amplitude change directly gives the time varying optical frequency tuning rate. The tuning rate is then integrated to obtain time varying optical frequency. The main advantage of our proposed method is the simplicity of the data processing blocks applied. We implemented our method to suppress nonlinear fre-

#107227 - $15.00 USD Received 5 Feb 2009; revised 24 Mar 2009; accepted 25 Mar 2009; published 26 Mar 2009

quency sweep in an OFDR and demonstrated highly effective spatial resolution enhancement of more than 30 times.

## 2. Principles of optical frequency measurement

In order to monitor the nonlinear frequency sweep of the TLS, we used an auxiliary interferometer (Mach-Zehnder configuration) whose schematic diagram is shown in Fig. 1.

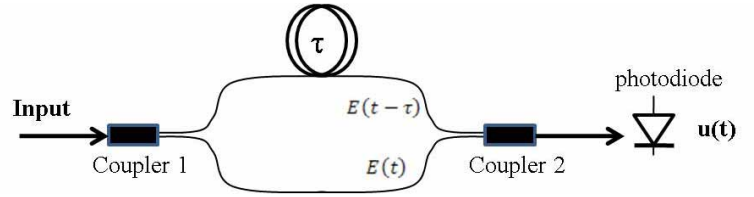


Fig. 1. Auxiliary interferometer layout

The electric field at the interferometer input (probe light) can be defined as

$$E(t) = E_0 \exp[j\phi(t)] \tag{1}$$

where $E_0$ is the amplitude of the electric field and $\phi(t)$ is the phase component. The phase component can be written as

$$\phi(t) = 2\pi \int_0^t \nu(u)\,\mathrm{d}u + \phi_0, \tag{2}$$

where $\phi_0$ is the initial phase ($t = 0$) of the light source and $\nu(t)$ is the instantaneous optical frequency of the laser. The probe light is divided into two waves at the first coupler which propagate along both arms of the interferometer having different lengths and then are recombined at the second coupler. The group delay difference between the two arms of the interferometer is known and denoted by $\tau$.

As the two waves arriving at the second coupler are derived from the same source, the intensity of the resulting electric field will be

$$\begin{aligned} I(t) &= \eta |E(t) + E(t-\tau)|^2 \\ &= 2\eta |E_0|^2 [1 + \cos(\phi(t) - \phi(t-\tau))] \end{aligned} \tag{3}$$

where $\eta$ is a constant that depends on the insertion loss of the two couplers. Equation 3 assumes the best case where the two incident fields have the same polarization. In general, a polarization controller is inserted in one arm of the interferometer to maximize the interference signal. It should be also noted that the optical path difference between the interferometer arms is much smaller than the coherence length of the laser source. The AC part of the interference signal detected at the photodiode is given by

$$u(t) = U_0 \cos(\phi(t) - \phi(t-\tau)) \tag{4}$$

where $U_0 = 2\eta\sigma|E_0|^2$ and $\sigma$ a constant that depends on the photodetector sensitivity. Next, by Taylor expanding the phase $\phi(t-\tau)$ about $t$ we obtain

#107227 - $15.00 USD Received 5 Feb 2009; revised 24 Mar 2009; accepted 25 Mar 2009; published 26 Mar 2009

$$\phi(t)-\phi(t-\tau)=2\pi\tau\nu(t)-2\pi\sum_{i=2}^{\infty}\frac{(-\tau)^i}{i!}\frac{\mathrm{d}^{i-1}\nu(t)}{\mathrm{d}t^{i-1}} \tag{5}$$

Then we neglect the second- and higher-order terms in Eq. 5 and substitute it in Eq. 4. In this case, Eq. 4 is simplified to

$$u(t)=U_0\cos\left(2\pi\tau\nu(t)\right). \tag{6}$$

This expression is valid when $\frac{\tau}{2\nu(t)}\frac{\mathrm{d}\nu(t)}{\mathrm{d}t}\ll 1$. From the detected signal $u(t)$ in Eq. 6, the optical frequency quantification can be obtained by applying the data processing steps schematically represented in Fig. 2.

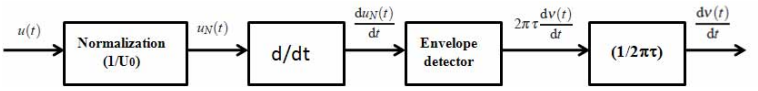


Fig. 2. Data processing steps

First of all, the detected signal is normalized. The normalized signal, $u_N(t)$ is obtained by dividing the $u(t)$ by its peak amplitude $U_0$. The time-varying optical frequency is then converted to amplitude variations by taking the differential of the normalized signal, $u_N(t)$

$$\frac{\mathrm{d}u_N(t)}{\mathrm{d}t}=-2\pi\tau\frac{\mathrm{d}\nu(t)}{\mathrm{d}t}\sin\left(2\pi\tau\nu(t)\right)=A(t)\sin\left(2\pi\tau\nu(t)\right). \tag{7}$$

Envelope detection of the sinusoidal signal represented in Eq. 7 permits therefore to obtain $A(t)$ which in turn yields the time-varying tuning rate ($\gamma(t)$) of the optical frequency as follows

$$\gamma(t)=\frac{\mathrm{d}\nu(t)}{\mathrm{d}t}=-\frac{A(t)}{2\pi\tau}. \tag{8}$$

Finally, the optical frequency variation can be determined with respect to the initial optical frequency by the integration of the obtained tuning rate in Eq. 8 as

$$\Delta\nu(t)=\int_0^t\gamma(u)\,\mathrm{d}u. \tag{9}$$

In spite of the fact that a derivative algorithm is employed to convert the optical frequency changes to intensity variations, our method shows rather good stability. This is due to the fact that the noise amplitude in our experiment set-up is quite low (about one percent of the interference signal amplitude).

So far, we have shown that the optical frequency variation with respect to time can be measured by using a self-homodyne interferometer and some data processing steps. Similar to previously published techniques [8, 10, 11], the optical frequency versus time has been deduced from the interference fringes of the auxiliary interferometer output by using mathematical manipulations. However, contrary to the previous ones, our new method uses only simple data processing steps and does not require to deal with complex numerical algorithms such as phase-unwrapping.

With this information, it is possible to suppress the effect of the nonlinear optical frequency sweep on the spatial resolution in a coherent OFDR set-up. The DUT is connected to the main (or test) interferometer in a conventional OFDR configuration and the detected signal is sampled at equidistant time intervals. The information of the measured optical frequency is used to

#107227 - $15.00 USD Received 5 Feb 2009; revised 24 Mar 2009; accepted 25 Mar 2009; published 26 Mar 2009

resample the output of the main interferometer with equidistant frequency intervals. In this way, the fast Fourier transform (FFT) algorithm commonly used to realize Fourier transform on the detected interference signal can be realized correctly as a function of the independent variable of interest, namely the instantaneous optical frequency.

## 3. Experimental set-up and results

The layout of the experimental OFDR system used to implement our swept-frequency measurement method is shown in Fig. 3. It comprises both the main (or test) interferometer including the DUT to be tested and an auxiliary interferometer which is used to determine the optical swept-frequency as a function of time as explained previously. The measured optical frequency is used to compensate the effect of nonlinear frequency sweep on the main interferometer's spatial resolution. The group delay mismatch between both arms of the auxiliary interferometer was $\tau = 12.8$ ns.

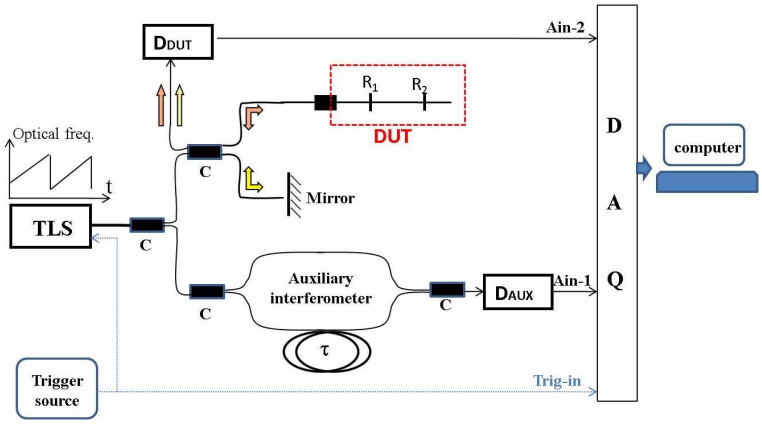


Fig. 3. OFDR system having auxiliary interferometer and main interferometer. (D: detector, C: coupler, DAQ: data acquisition card)

In the set-up, the TLS is a commercial external cavity laser (ECL) whose nominal tuning rate is set to about $\gamma_\nu = 1.25$ THz/s (about 1 nm sweep span over 100 ms sweep time) which means that the inequality $\frac{\tau}{2\nu(t)}\frac{d\nu(t)}{dt} \ll 1$ is satisfied for the given tuning range and Eq. 6 is valid. The optical power of the TLS was 0.1mW ·

For a given measurement, the outputs of the auxiliary and the main interferometers are acquired simultaneously on two analog input channels (Ain-1 and Ain-2 in Fig. 3) via the data acquisition card (DAQ) and are passed through the signal processing units represented in Fig. 2 by the computer. The operations of the DAQ and the TLS are triggered by an external TTL trigger source. Even though, the sawtooth sweep time of the TLS is 100 ms, the data acquisition uses a narrower acquisition time (time gate) in the FFT process. Time gate was about 40 ms. Therefore although the TLS optical frequency is swept over 1 nm, only about 0.4 nm of this range is used for the data acquisition. The best theoretical spatial resolution provided by the DAQ system is determined by the frequency-resolution bandwidth of the measurement system and is given by [12]

$$\Delta l = \frac{c}{2n_g\gamma}\Delta f \tag{10}$$

where the frequency sweep is assumed to be entirely linear with constant tuning rate ($\gamma$) , $c$ is the speed of light in vacuum, $n_g$ is the refractive group index of the DUT, and $\Delta f$ is the

#107227 - $15.00 USD Received 5 Feb 2009; revised 24 Mar 2009; accepted 25 Mar 2009; published 26 Mar 2009

frequency-resolution bandwidth of the system. In the ideal case of linear frequency modulation, the best spatial resolution in our system was about 0.2 cm considering the sampling rate of 0.4 MSample/s with 16384 sampling points at DAQ and constant tuning rate of 1.25 THz/s applied to the TLS.

The TLS is operated in sweep mode to ramp the optical frequency. But it shows unavoidable deviations from linear sweep during the measurement. Therefore, in our OFDR system, there is a spectral broadening due to the frequency sweep nonlinearities. This additional spectral broadening ($\Delta f_{NL}$) degrades the spatial resolution. In order to compensate this effect, the optical frequency deviation and tuning range are measured by using our method previously explained and the results are shown in Fig. 4. It is clear from Fig. 4-a that the optical frequency tuning rate is not constant but rather fluctuates around the applied tuning rate 1.25THz/s.

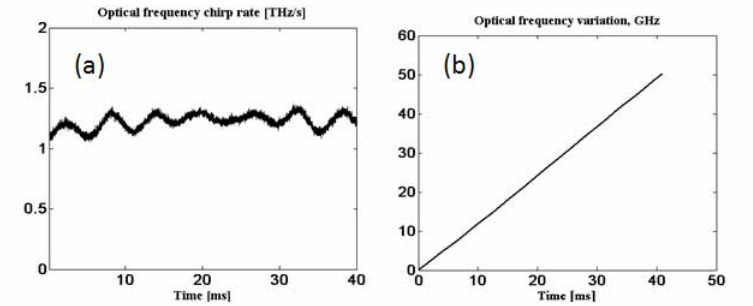


Fig. 4. (a) Measured time-varying tuning rate and (b) measured nonlinear optical frequency variation of a commercial TLS as a function of time.

The measured optical frequency-swept shown in Fig. 4-b is then used to compensate the effect of nonlinear sweep of the main interferometer. To produce a beat signal with equidistant optical frequency grid, we applied the following data processing steps. First, the measured optical frequency is interpolated (using spline data interpolation) so as to determine time points corresponding to equidistant optical frequency grid. Second, the beating signal from the main interferometer is re-sampled at these time points. Lastly, the re-sampled beating signal is converted to frequency domain using FFT algorithm. Therefore, the requirement of the FFT algorithm that data has to be sampled at equal intervals of the independent variable (optical frequency in our case, cf. Eq. 6) is satisfied, hence, the error due to nonlinear optical frequency sweep is eliminated.

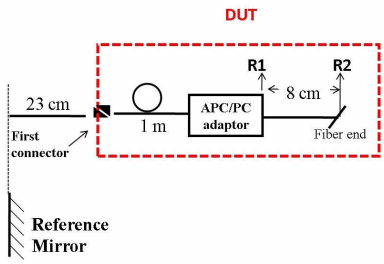


Fig. 5. Device Under Test in the OFDR system

In order to demonstrate our nonlinear frequency suppression approach, we applied our method to a conventional coherent OFDR set-up with a typical metrology application, namely testing discrete reflections coming from connectors and patchcords. The device under test for

#107227 - $15.00 USD Received 5 Feb 2009; revised 24 Mar 2009; accepted 25 Mar 2009; published 26 Mar 2009

the measurements is shown in Fig. 5. It consists of a 1 m-fiber, an FC/APC-FC/PC adaptor and FC/PC pigtail whose fiber-end is randomly cut. This configuration creates two strong reflections which are 8 cm-fiber apart (cf. Fig. 5). The OFDR spectra obtained with and without optical frequency linearization are presented in Fig. 6. As can be clearly seen in the figure, reflections R1 and R2 are blurred because of nonlinear optical frequency (Fig. 6-a) but are clearly resolved after the suppression of this effect by using our proposed method (Fig. 6-b).

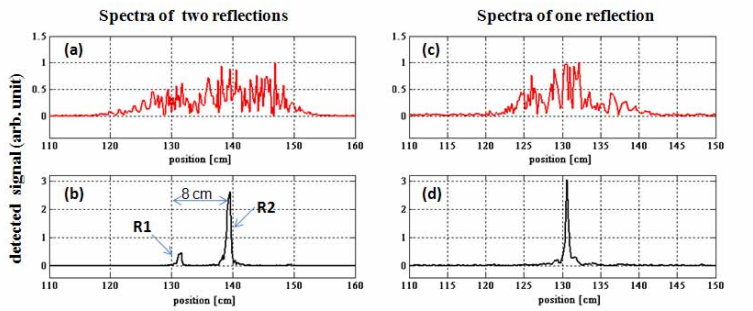


Fig. 6. Measured beat spectrum of the main interferometer having two reflections in the DUT (a) without (b) with the nonlinear optical frequency suppression, and having only one reflection in the DUT (c) without (d) with the nonlinear optical frequency suppression

As shown in Fig. 6-a, the beating signal is broadened over about 25 cm avoiding the two reflections to be distinguished. After linearizing the optical frequency, the spectrum becomes fine and the full with half maximum (FWHM) resolution on the reflection peaks becomes about 0.4 cm, which is close to the best spatial resolution of 0.2 cm.

In order to have a quantitative estimation of the resolution enhancement with the proposed technique, we repeated the experiment using only one reflection in the end of a 130 cm- sample fiber and keeping all the parameters of the system as defined before. The nonlinear frequency sweep results in the broadening of the beating signal over about 13 cm (Fig. 6-c). However, after using our nonlinear optical frequency suppression method, the FWHM resolution on the reflection peak becomes about 0.4 cm (Fig. 6-d) showing an enhancement of 30 times in spatial resolution.

The ratio of the improved spatial resolution to the fiber length in our system is 0.003 (0.4 cm/130 cm). Our method gives a similar result but uses simpler data processing steps when compared to the previously published method in the same category, where this ratio can be calculated as 0.006 (3 cm/5 m) [8].

## 4. Conclusion

In this paper we presented a new method for monitoring the nonlinear frequency sweep in high speed tunable laser sources. The monitoring system comprises a Mach-Zehnder interferometer and simple signal processing steps. By implementing simple data processing blocks, our method is able to measure optical swept-frequency in different kinds of tunable laser sources without any limitation in auxiliary interferometer length. We also successfully implemented our method to suppress nonlinear frequency sweep in a coherent OFDR and demonstrated spatial resolution enhancement of more than 30 times.

## Acknowledgments

This research was supported by Fonds de la Recherche Scientifique-Crédit aux Chercheurs (FNRS) and the Interuniversity Attraction Pole IAP 6/10 program of the Belgian Science Policy.

#107227 - $15.00 USD Received 5 Feb 2009; revised 24 Mar 2009; accepted 25 Mar 2009; published 26 Mar 2009